Environ Earth Sci (2012) 66:607–614
DOI 10.1007/s12665-011-1268-5

ORIGINAL ARTICLE

Understanding of the biochemical events in a chemo-bioreactor during continuous acid mine drainage treatment

Bidus Kanti Das · Santi M. Mandal · Jayanta Bhattacharya

Received: 3 December 2010 / Accepted: 20 July 2011 / Published online: 5 August 2011

Abstract Spent mushroom compost (SMC) is widely used as reactor matrix in passive bioreactor involving sulfate reducing bacteria (SRB) for acid mine drainage (AMD) treatment. Follow-up our previous report, recent work has been established the extent of activity, sustained organic carbon availability, and the biochemical events of successive alkalinity producing system-based chemo-bioreactor for continuous performance using SMC. Removal of iron and sulfate from influent was over 77 and 90%, respectively, for first 13 weeks, while sulfate removal efficiency suddenly dropped down to 31% thereafter. Ahead of 13th week, process failure was beginning to be noticed when available dissolved organic carbon (DOC) value dropped down to 50 mg/L. SRB population was mostly affected with DOC drought at this stage. Sulfur was one of the major elements found with other tested metals in blackish green effluent precipitate. Sulfide compounds of the tested metals were formed on both exhausted chemo-bioreactor bed and precipitate. FTIR analysis indicated that SMC was responsible for metal binding and available nutrients supply. The present study revealed the feasibility of SMC as a host for treating AMD by this chemo-bioreactor that will assist in designing the continuous treatment practice.

Electronic supplementary material The online version of this article (doi:10.1007/s12665-011-1268-5) contains supplementary material, which is available to authorized users.

B. K. Das · J. Bhattacharya (✉)
Department of Mining Engineering, Indian Institute of Technology Kharagpur, Kharagpur 721302, India
e-mail: jayantaism@gmail.com

S. M. Mandal
Central Research Facility, Indian Institute of Technology Kharagpur, Kharagpur 721302, India

Keywords Acid mine drainage · Fixed bed chemo-bioreactor · Spent mushroom compost · Sulfate reducing bacteria · Organic carbon drought · Biochemical events

Introduction

Acid mine drainage (AMD), characterized by high acidity (pH 2.0–4.0), high concentration of sulfate, metals and metalloids ions, is the creation of coal and metal mine industries mostly (Johnson and Hallberg 2005). It is a potential hazard to the environment, and the overall impact is to reduce ecological stability (Gray 1997). Hence, that should be treated before discharge.

Different technologies have been applied to mitigate the problem, in which biological treatment strategies using sulfate reducing bacteria (SRB) also find favor (Johnson and Hallberg 2005; Das et al. 2009). Under anaerobic condition, SRB oxidize organic compounds and reduce sulfate to hydrogen sulfide and thereby facilitate the precipitation of metal sulfides. Bicarbonate production in this reaction neutralizes the acidity. This type of bioremediation is generally achieved through anaerobic wetlands/compost bioreactors, permeable reactive barriers as well as in successive alkalinity producing system (SAPS) (Johnson and Hallberg 2005).

Limestone is often used to generate alkalinity in AMD treatment systems because of its low cost and availability to close proximity to mining areas. However, its effectiveness reduces when mainly Fe^{3+} of AMD precipitate, causing armoring and clogging. In SAPS, this problem is partially overcome as influent water flow vertically through organic layer, into limestone beds, and ultimately discharged (Demchak et al. 2001). In the organic layer (mainly compost), microbiological respiration removes

oxygen and produces the anaerobic zone where Fe^{+3} are reduced to Fe^{+2}. Fe^{+3} generally precipitate as pH rises, but Fe^{+2} are expected to be soluble at neutral pH. The reduced water then passes through limestone layer where the acidity is being neutralized.

Spent mushroom compost is widely used for the creation of organic layer in SAPS (Nairn and Mercer 2000; Demchak et al. 2001; Bhattacharya et al. 2008). It showed higher relative performance compared to other waste materials as electron donor for SRB (Chang et al. 2000). It can provide sufficient dissolved organic carbon (DOC), nitrogen (DON), and phosphate (Guo et al. 2001). Polysaccharide content of SMC is generally degraded by hydrolytic fermentative anaerobes to alcohols and fatty acids that support the growth of SRB (Chang et al. 2000). Because of its slow degradation rate and bulk physical property, it can be chosen as a suitable substrate for long-term operation in AMD bioremediation (Dvorak et al. 1992; Bhattacharya et al. 2008). SMC has also been applied for treating metals in AMD and coal mine drainage in passive bioreactor system (Dvorak et al. 1992; Stark et al. 1994). However, no systematic study has been carried out about its organic carbon–liberating capacity and to support SRB activity.

SAPS was reconstructed in the form of chemo-bioreactor and its performance to treat acidic and metal laden wastewater was reported in our previous study (Cheong et al. 2010). Spent mushroom compost was used as organic matrix in this study. However, the extent of nutrient supply and the biochemical aspects in such a setting is still unclear and is necessary for longer treatment process design. The objective of this study was to evaluate how long SMC could liberate available organic carbon, bacterial abundance (especially sulfate reducing bacteria) in this environment, and utilization of organic matrix. In addition, evaluation of limestone in terms of exhaustion for better performance of chemo-bioreactor in continuous treatment and the fate and the composition of metal precipitates have been analyzed.

Materials and methods

Chemo-bioreactor operation

The study was performed with a pilot-scale gravity fed chemo-bioreactor system reported earlier (Cheong et al. 2010). SMC and limestone were reported to be characterized for alkalinity generation, DOC liberation, and metal release. The source of the materials used in this study was exactly the same as earlier. The amount of these material and some parametric values of synthetic AMD was slightly modified. Main reacting tank D (145 × 30 cm) of the chemo-bioreactor was packed with 4.8 kg of limestone (4.2 cm) at the base followed by 5.12 kg of SMC (14 cm) and a gravel layer (made up of quartz type of rock) of 5.3 kg (3.5 cm) at the top, with a final reacting bed height of 21.7 ± 0.2 cm. The mass density of the reactor bed was 0.77 g cm^{-3}. The porosity was calculated to be 0.59 ± 0.01, using the final reacting bed volume (without gravel layer) and the calibrated liquid volume used to pack the bed. The chemo-bioreactor was operated in room temperature at 25 ± 5°C. Synthetic acid mine drainage was prepared alike the previous study. The recipe was based on reported literature values of originally characterized AMD. It contains metal ions (mg/L) Fe (460), Mn (220), Mg (267) Cu (264), and SO_4^{2-} (2,611) with pH 2.8 and acidity of 8 mg/L as CaCO3. All chemicals used to prepare solutions were reagent grade. Eighty liters of this mixture solution was fed to the chemo-bioreactor (D) initially, filling other three tanks (A, B and C), and was left to settle. Blackish pond sediment (80 mL) having most probable number (MPN) of 48 ± 4 SRB cells/100 mL was added as inoculums. After 15 days, continuous flow was started. A flow rate of 535.7 mL/h (0.0706 h^{-1} dilution rate with respect to liquid volume) was maintained during the experiment, which is equal to 0.758 cm h^{-1} of superficial flow velocity and with a hydraulic retention time of 24 h through the bed. During this period, the water volume was kept constant by controlling flow rate until end (18 weeks).

Sampling and analysis

Influent (sample port in tank D) and effluent (tank F) water were collected at 7 days interval regularly. Samples for analytical purpose were filtered through a 0.45-μm nylon membrane filter to remove precipitates and other solid materials. Metal concentrations were measured by ICP-MS (Varian 820-MS) after pretreatment with concentrated HNO_3 (1.5 μl/mL sample; v/v) (Greenberg et al. 1992). Sulfate was measured by titration method in electrometric auto-titrator (Orion 950 Ross FASTQC, USA) in the fixed millivolt (mv) increment mode for first-derivative endpoint detection. pH and oxidation reduction potential (ORP) were measured by multi-parameter water analyzer (Orion 5–Star BENCHTOP MULTI, Thermo Scientific, USA). Total organic carbon (TOC) was analyzed by TOC analyzer (TOC-V CPH, Shimadzu, Japan) using the filtered sample and reported as DOC (Khan et al. 1998). Limestone exhaustion in terms of calcium ion concentration was measured before and after the experiment. Whenever possible, pH, metals, and sulfate were determined on the same day the samples were collected. Total bacterial count of the reactor matrix was performed by standard plate count method on Trypticase soy agar. SRB count of the matrix was done by MPN method described by Fortin et al.

(2000). Reactor matrix was taken during sampling, weighted, and diluted into respected dilution before plating or MPN experiment. Total bacterial population is expressed in CFU/g matrix, whereas SRB population is expressed in MPN/g matrix (Cochran 1950). Epifluorescence microscopic method was performed for observing bacterial morphology and live-dead differentiation (Leica DMR coupled with Leica MPS60 photomicrographic system). In brief, 1 g of matrix was homogenized in 100 mL 1x PBS buffer. One and half milliliter of it was centrifuged for 5,000 rpm × 3 min, and supernatant was discarded. The pellet was dissolved in 1 mL PBS buffer and again centrifuged under similar condition. Acridine orange (AO) and propidium iodide (PI) of 2 µl each were added to the pellet, and volume was adjusted to 25 µl by 1x PBS buffer. The tubes were then incubated for 20 min at dark. After incubation, the stains were washed thrice with PBS buffer and then centrifuged for 4 min at 5,000 rpm to pellet the cells. The pellet was dissolved again in PBS buffer to make the volume 500 µl. Living bacterial produce green fluorescence (due to AO), and dead would produce red (due to PI). The counting was done by standard procedure (Mesa et al. 2003)

SMC and precipitate analysis

SMC samples (before and after experiment) and the precipitate formed in the E tank were analyzed for precipitate characterization. Samples were examined by a Zeiss field emission scanning electron microscope (FESEM) with attached energy dispersive X-ray (EDAX) analyzer. Mineral phases were identified by X-Ray Diffractometry (XRD) (Philips) with CuKα radiation ($\lambda = 1.5406$). Peaks were identified by standard software (JCPDS-ICDD 1999). Infrared spectra of SMC and precipitates were recorded on a Nexus TM 870 FT-IR (Thermo Nicolet, USA) spectrophotometer equipped with deuterated triglycine sulfate detector thermo electric cool (DTGS TEC). Each sample spectra was performed using KBr disc in the range 400–4,000 cm^{-1}.

Results

Chemo-bioreactor performance

Figure 1 shows the time course of removal efficiency of all tested metals (Fe, Mn, Mg, and Cu), and the average reactor performance is summarized in Table 1. Removal of metal ions in the effluent was found to be started from 3rd week, but the value of Mg reduction percentage was negative, indicating its initial addition into the effluent (Fig. 1). Magnesium was the least reduced metal compared to other tested metals, while Cu was reduced maximum in the same time. Mg (93.6%) and Mn (96.4%) were reduced maximum at 3rd week, Cu (97.3%) at 6th week, Fe (97.9%), and sulfate (98.6%) at 12th week of chemo-bioreactor performance. The pH was maintained over 6- up to

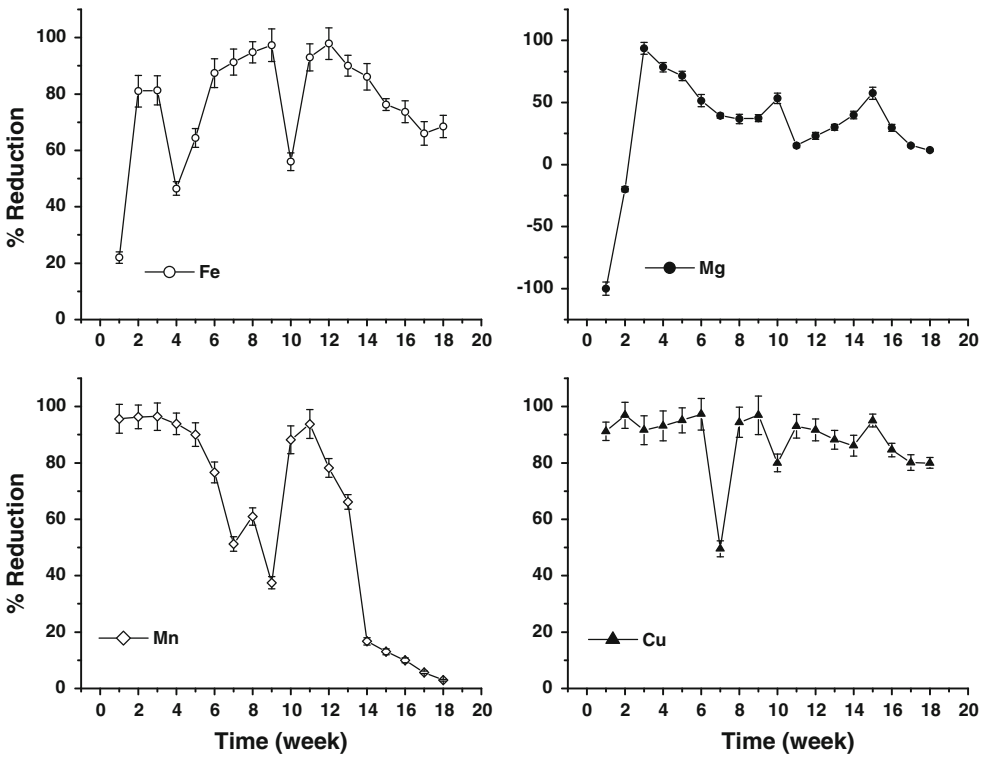

Fig. 1 Status of metal concentration during continuous flow. Data are the mean of triplicates performance result ± standard error of the mean (S.E.M.)

Table 1 Chemo-bioreactor performance during continuous operation

Removal efficiency (%)					DOC in chemo-bioreactor (mg/L)
SO_4	Fe	Mn	Cu	Mg	
87.5 ± 2.74	77.79 ± 2.12	74.4 ± 1.98	88.9 ± 1.44	32.14 ± 1.22	244.07 ± 11.65

Data are the mean of average result up to 14th week ± S.E.M

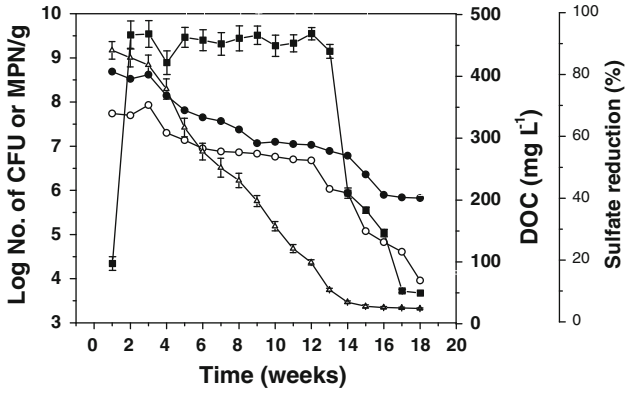

Fig. 2 Relation of sulfate reduction with available DOC and bacterial load. Symbol indicates DOC (*open triangle*); Sulfate (*filled square*); total bacterial population (*filled circle*); and sulfate reducing bacterial population (*open circle*), and data are the mean of triplicates performance result ± S.E.M

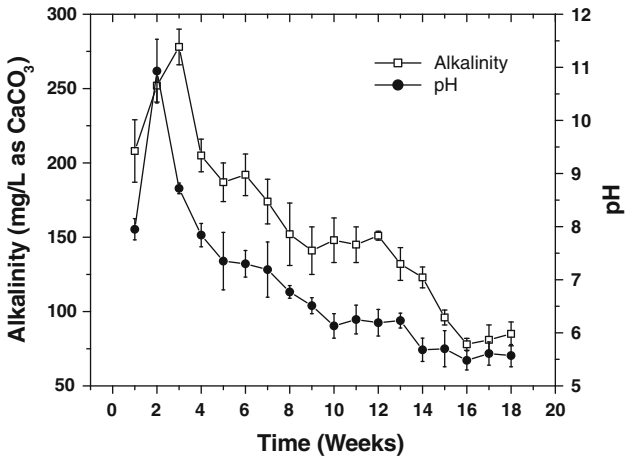

Fig. 3 pH and alkalinity profile during continuous run. Data are the mean of triplicates performance result ± S.E.M

13-week period. ORP was less than −100 mV during the experiment. However, removal of all tested metals and sulfate was decreased sharply after 14th week, indicating some kind of process failure occurred at this stage (Figs. 1 and 2). DOC level was also dropped from 400 to 50 mg/L after 14th week (Fig. 2). Drop of alkalinity after 12th week and pH after 13th week was also found (Fig. 3). Calcium remained in the exhausted limestone is 36.93 ± 0.68%, implying about 63% was used.

Bacterial abundance

Double fluorescence stained samples (Fig. S1) showed both live and dead cells were present in the effluent, in which rod-shaped cells were predominated. Figure 2 illustrates the status of total bacterial and SRB population density in the chemo-bioreactor. Throughout the experiment, both population was found to be declined except at 3rd week when SRB ($\approx$108 MPN/g) as well as total bacterial population ($\approx$109 CFU/g) reached maximum. Results indicate that initially there was a prevalence of other bacteria over SRB in the chemo-bioreactor. Gradually, growth of SRB predominated, and hence, SRB population curve follows the same pattern like total bacterial population. From 9th to 12th week, SRB population began to comprise most of the bacterial population and at this period, total bacterial population was 1.73 and 2.5 times of SRB population, respectively. Total bacterial population was far over 107 CFU/g, whereas SRB population was near 107 MPN/g at DOC higher than 100 mg/L. However, both total bacterial and SRB population decreased exponentially after 12th and 14th week when available DOC level was as low as 99 and 35 mg/L, respectively. Noticeably, at that point, SRB population decreased sharply correlating significantly with released DOC level. SRB population dropped down to 104 MPN/g at DOC level less than 50 mg/L, at the end of the experiment comparing a constant population of total bacteria near 106 CFU/g at that period.

Microscopic and mineralogical analysis

SEM images of SMC samples before and after the experiment (exhausted SMC) revealed structural differences (Fig. 4). Biofilm formation on the SMC bed was observed after experiment. Attached EDAX analysis demonstrates that the major elements in SMC before loading were Si, Al, Mn, Fe, Mg, and O (H is not detectable) and minor elements included Cu, C, and K. Major elements in exhausted SMC were Si, Fe, Ca, and O, whereas minor elements being Cu, Mg, and Al. Blackish green precipitates were formed in the first effluent tank (E) from the beginning of the experiment and continued to form till the completion of the experiment. SEM analysis of the precipitates (Fig. 4c) shows the formation of some geometrical-shaped particles associated intermittently with organic matter in low

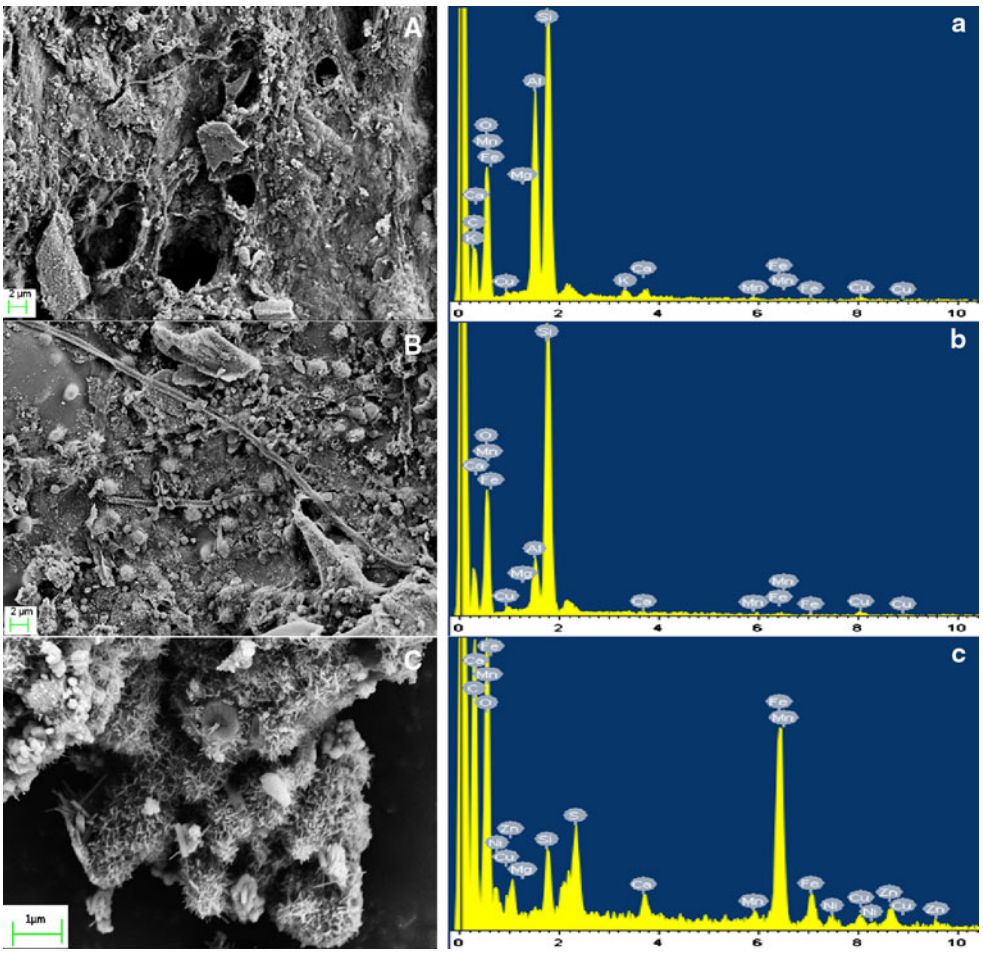

Fig. 4 SEM and EDAX analysis of SMC and precipitates. SEM and EDAX micrograph of samples, respectively, (*A* and *a*) SMC before loading, (*B* and *b*) SMC after experiment, and (*C* and *c*) precipitates in effluent tank

concentration. Major elements of this precipitates were Fe, Mn, Ca, C, S, and O and minors were Si, Cu, Mg, Zn, and Ni.

No sulfide mineral has been detected in the powder XRD spectra of raw SMC (Fig. 5). However, sulfide compound of all tested metals has been recognized in exhausted SMC. This sample contains digenite (Cu_9S_5), magnesium sulfide (MgS), manganese oxide (MnO), iron sulfide (FeS), mackinawite (FeS), hausmannite (Mn_3O_4), and periclase (MgO). Precipitates formed in the effluent tank were predominantly sulfides, namely iron sulfide (FeS), pyrite (FeS_2), magnesium sulfide (MgS), hauerite (MnS_2), greigite (Fe_3S_4), covellite (CuS), and manganese sulfide (β-MnS).

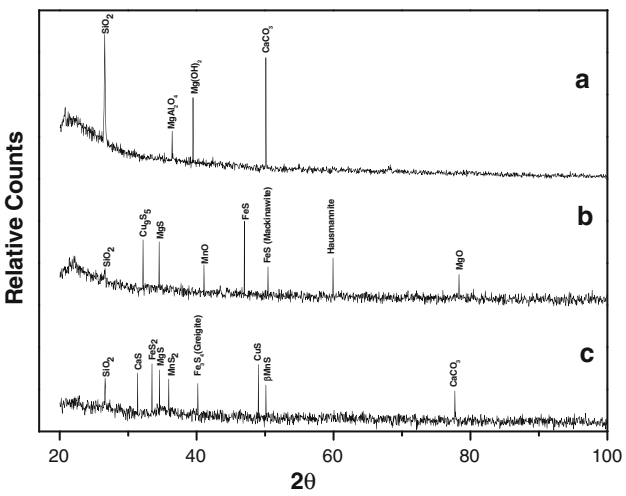

Fig. 5 X-ray diffraction pattern of SMC and precipitates. Diffraction pattern of **a** SMC before loading; **b** SMC after experiment; and **c** precipitate formed in the effluent tank

FTIR analysis

FTIR spectrum (Fig. 6) of raw and exhausted SMC and effluent tank precipitate showed broad peaks at 3,418,

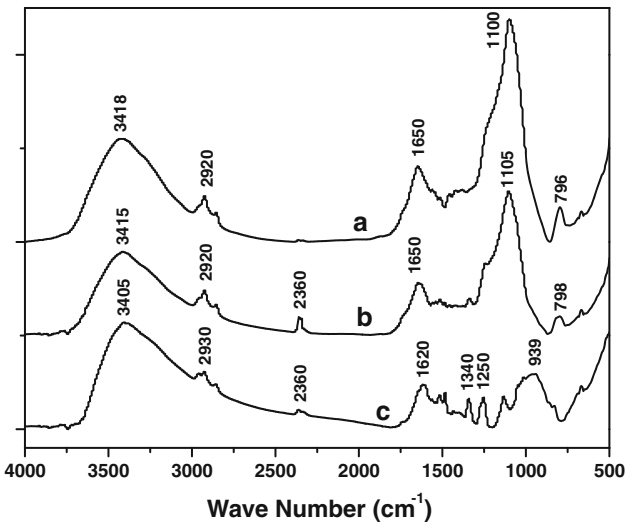

Fig. 6 Overlaid FTIR spectra of SMC and precipitates. **a** Control SMC before loading to experimental tank; **b** SMC after experiment showed new peak at 2,360 cm^{-1} (presence of CO_2) and decrease in peak intensity near 1,100 cm^{-1} (utilization of secondary alcohol), and **c** precipitate formed in the effluent tank showed along with CO_2, new peaks formed at 1,252 and 1,345 cm^{-1} representing SO_3 stretching

3,415, and 3,405 cm^{-1}, respectively, corresponding to the OH stretching of polymers or phenolic group and N–H stretching of primary amides that might be associated with cellulosic cell wall of mushroom and plant debris (Bellamy 1975; Lau et al. 2003; Chen et al. 2005). Decrease in intensity of peak near 3,400 cm^{-1} in exhausted SMC can be attributed to the involvement of the H-bonded OH and N–H group in metal biosorption. Shifting of peak in the region of 1,650 cm^{-1} [C=O stretching of primary amide] (Bellamy 1975; Pagnanelli et al. 2000) of SMC to lower frequencies at 1,620 cm^{-1} in effluent precipitate can be due to interaction of this group with metal ions. Peaks near 1,100 cm^{-1} [C=O; stretching and O–H deformation vibration of secondary alcohol] (Bellamy 1975) are present in both SMC sample but absent in precipitates. A new peak with small intensity at 2,360 cm^{-1} region in sample of exhausted SMC and precipitate was found [υ3 band of CO_2] (Nakamoto 1986; Taraschewski et al. 2005). New peaks in precipitate at 1,252 and at 1,345 cm^{-1} can be assigned to SO_3 stretching, (Winie and Arof 2006; Kang et al. 2007) and inorganic NO_2 stretching (Bellamy 1975), respectively. It seemed the deposition of sulfate ions also occurred with metal ions. No perceptible change of the peak position and intensity at 2,920 cm^{-1} (the peak signifying CH_2 asymmetric stretch in aromatic and alkenes present in lignin) in exhausted SMC was found (Bellamy 1975). Absorption peaks at 796, 798, and 939 cm^{-1} in raw SMC, exhausted SMC and in precipitate, respectively, could be due to the presence of residual quartz (Snyder et al. 1983; Misaelides et al. 1996; Han-xu et al. 2008).

Discussion

The results illustrate that a total 1,620 liters of synthetic AMD has been treated successfully during long-term running. This treatment process was established as a cost effective scheme in previous study (Cheong et al. 2010), and SMC used to water treated ratio was much less (3.16 g SMC used/liter AMD treated) in this study. Iron and sulfate removal efficiency was better than other reported chemo-bioreactor (Dvorak et al. 1992; Stark et al. 1994; Demchak et al. 2001). However, reduction in Mg was limited in as much to reach the expected level compared to other metals, even some addition of it to the effluent also observed. Mineralogical study shows the presence of magnesium compound in effluent tank precipitate (Figs. 4c and 5c). In our previous study, we have shown that SMC releases Mg in similar condition (Cheong et al. 2010). From these observations, it can be stated that both addition of Mg from SMC and its transformation to insoluble complexes in the chemo-bioreactor occurred simultaneously. Deposition of metals onto bacterial cell or in cell-bound polysaccharide is a well-known phenomenon (Iyer et al. 2005). Functional groups such as carboxylic, amino, thiol, hydroxyl, and hydroxy-carboxylic groups present in bacterial cell wall are reported to interact with metal ions (Sigg 1987). Phenolic group takes a major part of metal deposition which was often found in microbes and distributed widely in the lignin, cellulose, and semi-cellulose containing fungal cell wall (Chen et al. 2005). Metal sorption by various organic groups treating AMD is reported earlier (Gibert et al. 2005). FTIR analysis shows the involvement of OH group of polymers or phenolic compounds, N–H and C=O group of primary amides, in metal binding. It may be hypothesized that metal ions are deposited onto the SMC and bind to its phenol-rich constituent and cell walls of bacteria. Periodic fluctuations of the metal removal as shown in Fig. 1 were probably due to the simultaneous adsorption–desorption of metals into the matrix. Formation of biofilm on SMC from SEM images and presence of SRB by MPN test have been established here. FTIR study reveals the presence of CO_2 in exhausted SMC and precipitate, and those points toward either microbial metabolism-evolved-CO_2 in the chemo-bioreactor or residual limestone-evolved-CO_2 in precipitate. No significant change was observed of the peak position, and intensity remained at 2,920 cm^{-1} in exhausted SMC. Therefore, it can be ascribed that lignin of SMC was neither utilized as nutrient source nor responsible for biosorption or it might only be used as microstructure for attachment site of microbes.

XRD analysis of both exhausted SMC and precipitates revealed the presence of sulfide complex of all tested metals. Diverse SRB species are reported to be present in sulfidogenic reactor feeding simple organic carbon source

(Sigg 1987; Gibert et al. 2005). Majority and diversity of metal sulfide formations in effluent precipitate (Fig. 5c) indicate the diverse mechanism of sulfate reduction in the reactor. There is a high likelihood of SRB-mediated H_2S production, and thus metal sulfide formation could constitute the major reactions.

Solubility of metal sulfides was highly reduced at pH 5.0–9.0 and hence got precipitated. There is a positive correlation between SRB abundance and sulfate reduction. At primary stage of continuous flow when adequate DOC was present in the chemo-bioreactor, total bacterial population was nearly tenfold greater than SRB at 9th week, whereas this difference became very close after that. FTIR data showed that (decrease in band intensity at 1,100 cm^{-1} in exhausted SMC compared to raw SMC) microorganism in the chemo-bioreactor could have utilized the alcoholic group in SMC for their growth. SRB are only able to utilize complex organic carbon when synergic effect of other species results SRB degradable one (Neculita et al. 2007; Zagury et al. 2006). Therefore, initially there might be diverse microbial species including some aerobes present, which provided available organic carbon to SRB by synergic action. Microbial metabolism led CO_2 and limestone-evolved-CO_2 below the long water column helped to make the environment anoxic and supported anaerobic microbial growth. Negative ORP value confirms the oxygen deficient condition during the experiment. When steady state condition was being established, sulfate became the major electron acceptor and SRB might outcompete other microbes, as they have a thermodynamic advantage in sulfate-rich condition (Fernandez-Polanco and Garcia Encina 2006; Neculita et al. 2007).

After 13th week, a process failure of chemo-bioreactor was observed. It might be due to the lower level of DOC and this reduced DOC level contributed to the reduction in SRB abundance. However, at that time, total bacterial count was not reduced as rapidly as SRB. This is might be due to the exhaustion of SRB degradable DOC. However, released DOC was sufficient to promote the growth of other bacteria present at that stage. Sulfate reduction in the chemo-bioreactor dropped abruptly with falling DOC level. Therefore, a drought of degradable organic carbon for SRB started to occur after 13th week. In the absence of sufficient electron donors, metabolism of SRB stopped and growth ceased resulting population decrease. An enormous fall of alkalinity and slight drop of pH might be due to the cessation of microbial alkalinity. Sudden change of alkalinity is reported to be results on the change of microbial community in sulfidogenic reactor (Zhao et al. 2010). That may be a reason of less effect on total microbial population after 13th week. Whatever little amount of metal sulfide was formed at this stage became soluble at that pH. Hence, organic carbon drought and insufficient alkalinity in chemo-bioreactor caused process failure. SRB degradable organic carbon dosing after that instance can be thought as a sustainable treatment solution at large scale and longer treatment.

Conclusion

The developed pilot scale SAPS-based chemo-bioreactor showed better performance for long-term AMD treatment than other earlier developed. SMC used was a good host for SRB growth and activity. However, unavailability of DOC after some instance was the major reason for process failure combined with restricted alkalinity in the chemo-bioreactor. In addition to that, SMC is a good absorbent for direct metal removal also. Hence, the developed chemo-bioreactor is cost effective and useful for long-term AMD treatment with better performance.

Acknowledgments This work was funded by Indian Institute of Technology Kharagpur, India. The authors are grateful to K. Mohan (IIT Kharagpur, India) for helping in TOC analyses.

References

Bellamy LJ (1975) The infrared spectra of complex molecules. Chapman and Hall, London

Bhattacharya J, Ji SW, Lee HS, Cheong YW, Yim GJ, Min JS, Choi YS (2008) Treatment of acidic coal mine drainage: design and operational challenges of successive alkalinity producing systems. Mine Water Environ 27(1):12–19

Chang IS, Shin PK, Kim BH (2000) Biological treatment of acid mine drainage under sulphate-reducing conditions with solid waste materials as substrate. Water Res 34(4):1269–1277

Chen GQ, Zeng GM, Tu X, Huang GH, Chen YN (2005) A novel biosorbent: characterization of the spent mushroom compost and its application for removal of heavy metals. J Environ Sci (China) 17(5):756–760

Cheong YW, Das BK, Roy A, Bhattacharya J (2010) Performance of a SAPS based chemo-bioreactor treating acid mine drainage using low doc spent mushroom compost and limestone as substrate. Mine Water Environ 29:217–224

Cochran WG (1950) Estimation of bacterial densities by means of the most probable number. Biometrics 6(2):105–116

Das BK, Roy A, Koschorreck M, Mandal SM, Wendt-Potthoff K, Bhattacharya J (2009) Occurrence and role of algae and fungi in acid mine drainage environment with special reference to metals and sulfate immobilization. Water Res 43(4):883–894

Demchak J, Morrow T, Skousen J (2001) Treatment of acid mine drainage by four vertical flow wetlands in Pennsylvania. Geochem Explor Environ Anal 1(1):71–80

Dvorak DH, Hedin RS, Edenborn HM, Mclntire PE (1992) Treatment of metal-contaminated water using bacterial sulfate reduction: result from pilot scale reactors. Biotechnol Bioeng 40(5): 609–616

Fernandez-Polanco M, Garcia Encina P (2006) Application of biological treatment system for sulfate rich wastewater. In: Cervantes F, Pavlostathis S, van Haandel A (eds) Advanced

biological treatment processes for industrial wastewaters. IWA publishing, London, pp 215–218

Fortin D, Roy M, Rioux JP, Thibault PJ (2000) Occurrence of sulfate-reducing bacteria under a wide range of physico-chemical conditions in Au and Cu-Zn mine tailings. FEMS Microbiol Ecol 33:197–208

Gibert O, de Pablo J, Cortina JL, Ayora C (2005) Sorption studies of Zn(II) and Cu(II) onto vegetal compost used on reactive mixtures for in situ treatment of acid mine drainage. Water Res 39:2827–2838

Gray NF (1997) Environmental impact and remediation of acid mine drainage: a management problem. Environ Geol 30:62–71

Greenberg AE, Clesceri LS, Eaton AD (1992) Standard methods for the examination of water and waste water, 18th edn. American Public Health Association, Washington DC

Guo M, Chorover J, Rosario R, Fox RH (2001) Leachate chemistry of field—weathered spent mushroom substrate. J Environ Qual 30:1699–1709

Han-xu L, Xiao-sheng Q, Yong-sin T (2008) Ash melting behaviour by Fourier transform infrared spectroscopy. J China Univ Min Technol 18:245–249

Iyer A, Mody K, Jha B (2005) Biosorption of heavy metal by a marine bacteria. Mar Pollut Bull 50:340–343

Johnson DB, Hallberg KB (2005) Acid mine drainage remediation options: a review. Sci Total Environ 338:3–14

Kang SY, Lee JU, Kim KW (2007) Biosorption of Cr(III) and Cr(VI) onto the cell surface of *Pseudomonas aeruginosa*. Biochem Eng J 36:54–58

Khan E, Babcock RW Jr, Stenstrom MK, Suffet IH (1998) Method development for measuring biodegradable organic carbon in reclaimed and treated wastewaters. Water Environ Res 70: 1025–1032

Lau KL, Tsang YY, Chiu SW (2003) Use of spent mushroom compost to bioremediate PAH-contaminated samples. Chemosphere 52:1539–1546

Mesa MM, Macias M, Cantero D, Bajra F (2003) Use of the direct epifluorescent filter technique for the enumeration of viable and total acetic acid bacteria from vinegar fermentation. J Fluoresc 13:261–265

Misaelides P, Godelitsas A, Link F, Baumann H (1996) Apllication of the 27Al (p, γ)28 Si nuclear reaction of the characterization of the near-surface layers of acid-treated HEU-type zeolite crystals. Microporous Mater 6:37–42

Nairn RW, Mercer MN (2000) Alkalinity generation and metals retention in a successive alkalinity producing system. Mine Water Environ 19:124–133

Nakamoto K (1986) Infrared and Raman spectra of inorganic and coordination compounds. Wiley, New York

Neculita CM, Zagury GJ, Bussiere B (2007) Passive treatment of acid mine drainage in bioreactors using sulfate-reducing bacteria: critical review and research needs. J Environ Qual 36:1–16

Pagnanelli F, Papini MP, Trifoni ML, Vegli F (2000) Biosorption of metal ions on *Arthrobacter* sp.: biomass characterization and biosorption modeling. Environ Sci Technol 34:2773–2778

Sigg L (1987) Surface chemical aspects of the distribution and fate of metal ions in lakes. In: Stumm W (ed) Aquatic surface chemistry: chemical processes at the particle-water interface. Wiley, New York, pp 319–349

Snyder RW, Painter PC, Cronauer DC (1983) Development of FT-i.r. procedures for the characterization of oil shale. Fuel 62:1205–1214

Stark LR, Wenerick WR, Williams FM, Stevens SE Jr, Wuest PJ (1994) Restoring the capacity of spent mushroom compost to treat coal mine drainage by reducing the inflow rate: a microcosm experiment. Water Air and Soil Pollut 75:405–420

Taraschewski M, Cammenga HK, Tuckermann R, Bauerecker S (2005) FTIR study of CO and HO/CO nanoparticles and their temporal evolution at 80 K. J Phys Chem A Mol Spectrosc Kinet Environ Gen Theory 109:3337–3343

Winie T, Arof AK (2006) FT-IR studies on interactions among components in hexanoyl chitosan-based polymer electrolytes. Spectrochim Acta A 63:677–684

Zagury GJ, Kulnieks VI, Neculita CM (2006) Characterization and reactivity assessment of organic substrates for sulphate-reducing bacteria in acid mine drainage treatment. Chemosphere 64:944–954

Zhao YG, Li XW, Wang JC, Bai J, Tian WJ (2010) Performance of a sulfidogenic bioreactor and bacterial community shifts under different alkalinity levels. Bioresour Technol 101:9190–9196